JACS
JOURNAL OF THE AMERICAN CHEMICAL SOCIETY

Communication

pubs.acs.org/JACS

Enhanced Electrogenerated Chemiluminescence in Thermoresponsive Microgels

Florent Pinaud, Lorenzo Russo, Sandra Pinet, Isabelle Gosse, Valérie Ravaine,* and Neso Sojic*

Institut des Sciences Moléculaires, CNRS UMR 5255, University of Bordeaux, ENSCBP. 33607 Pessac, France

Supporting Information

ABSTRACT: The electrochemistry, photoluminescence and electrogenerated chemiluminescence of thermoresponsive redox microgels were investigated. For the first time, reversible ECL enhancement is demonstrated in stimuli-responsive 100-nm microgel particles. Such an unexpected amplification reached 2 orders of magnitude, and it is intrinsically correlated with the collapse of the microgel particles. The swell−collapse transition decreases the average distance between adjacent redox sites and favors the electron-transfer processes in the microgels resulting in the enhanced ECL emission.

Electrogenerated chemiluminescence (ECL) is the process of light emission by the excited state of a luminophore that results from an initial electrochemical reaction at the electrode surface.[1] ECL is a remarkably versatile and ultrasensitive method that has emerged in various research fields.[1b] To increase the sensitivity and the multiplexing performances of ECL, many efforts have been focused on the development of novel strategies and of new ECL nanoemitters with very innovative results reported at the nanoscale.[2] For example, a seminal approach based on nanocrystal quantum dots has been reported for efficient ECL generation.[2b]

Particularly fascinating nanomaterials are stimuli-responsive hydrogel particles, or microgels. The properties of such so-called "smart" microgels are modulated by an external stimulus (e.g., temperature, pH, biomolecular recognition, light, etc.), which triggers expansion or contraction of the polymer network, at the origin of sensing capabilities.[3] So far, many luminescent microgels have been reported that are capable of transducing these swelling variations into a change in fluorescence intensity, via polarity-sensitive fluorophores,[4] fluorescence resonance energy transfer (FRET)[5] or fluorescence quenching of quantum dots.[6] Similarly to other thermoresponsive luminescent nanomaterials,[7] such systems have been successfully used for optical measurement of intracellular temperature.[4] However, examples of electrochemically active microgels are scarce, although responsive polymers have gained an increasing interest over the past years.[8] The combination of ECL with stimuli-responsive microgels offers the opportunity to design novel nanoparticles whose ECL signal is manipulated not only by the electrode potential but also by an external stimulus. In addition, they would be very useful for bioanalytical applications since such microgels may improve the sensitivity[9] and also increase the complexity of the assays by playing with different stimuli.[6b,10] Herein, through a rational choice of model ECL and stimuli-sensitive microgel systems, electrochemistry and ECL of thermoresponsive 100-nm microgels are reported for the first time, and we demonstrated an unexpected enhancement of the ECL signal, which occurs at the swell−collapse transition of the microgel particles.

We selected prototypical thermoresponsive microgels based on polyalkylacrylamide derivatives, such as poly(*N*-isopropylacrylamide) (pNIPAM). These hydrogel particles are swollen in water below the so-called volume phase transition temperature (VPTT) and shrink when heated above it because of a change in the polymer−solvent affinity. To manipulate the VPTT, we modified the chemical functions R_1 and R_2 on the polymeric chains (Figure 1).[11] Monodispersed microgels with different

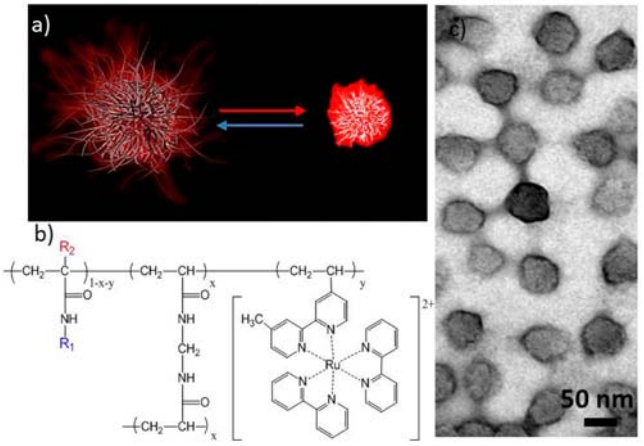

Figure 1. (a) Schematic representation of the thermoresponsive ECL microgels in the swollen (left) and collapsed (right) states. (b) Chemical structure of the cross-linked microgels with different chemical groups R_1 and R_2. (c) Transmission electron microscopy image of dried microgels.

VPTT were employed as the polymer matrix to covalently attach the ECL luminophore (Table S1, Supporting Information).[12] The hydrodynamic diameter of pNIPAM-1 was measured in PBS by dynamic light scattering (DLS) revealing a value of 130 nm in the swollen state below its VPTT, which is 33 °C (Table S1, Supporting Information). When the temperature is raised above the VPTT, the microgel collapses and the diameter of the particles decreases to 65 nm.

Received: January 29, 2013
Published: March 29, 2013

   dx.doi.org/10.1021/ja401011j | *J. Am. Chem. Soc.* 2013, 135, 5517−5520

Photoluminescence (PL) spectra of the microgel shows an emission at 610 nm, which is typical for the metal-to-ligand charge transfer (MLCT) transition of the $Ru(bpy)_3^{2+}$ complex (Figure S1, Supporting Information). It confirms the successful grafting of the ruthenium complex to the pNIPAM matrix. By increasing the temperature from 20 to 50 °C, PL spectra of the microgel show a monotonic decrease of the intensity without any shift of the emission wavelength (Figure S1, Supporting Information). The decrease is related to the classic temperature quenching of the PL.[13] An increase of 10 °C provokes a constant PL loss of 11% similarly to free $Ru(bpy)_3^{2+}$ in water. But the gel collapse has no specific effect on the PL of the pNIPAM-1 microgel.

The microgels were further characterized by differential pulse voltammetry (DPV). Microgels exhibit a well-defined oxidation peak at 1.14 V (Figure S2, Supporting Information). The redox centers or a fraction of them are therefore electrochemically accessible in the microgels, and their oxidation potential is identical to those of free $Ru(bpy)_3^{2+}$. The ECL of the pNIPAM-1 microgels was examined using three anodic coreactant species: tri-*n*-propylamine (TPrA),[14] 2-(dibutylamino)ethanol (DBAE)[15] and oxalate.[16] We selected them because they are either negatively or positively charged in PBS. In addition, they follow completely different mechanisms to generate ECL. A steady-state ECL intensity is obtained with TPrA below and above VPTT. Furthermore, ECL spectra of the microgels in the swollen and collapsed states (Figure S3, Supporting Information) are identical to PL spectra. The same excited state is generated below and above VPTT upon electrochemical and photochemical excitation.

Figure 2a shows the cyclic voltammograms of pNIPAM-1 in the presence of 10 mM TPrA at 25 and 37 °C. The first

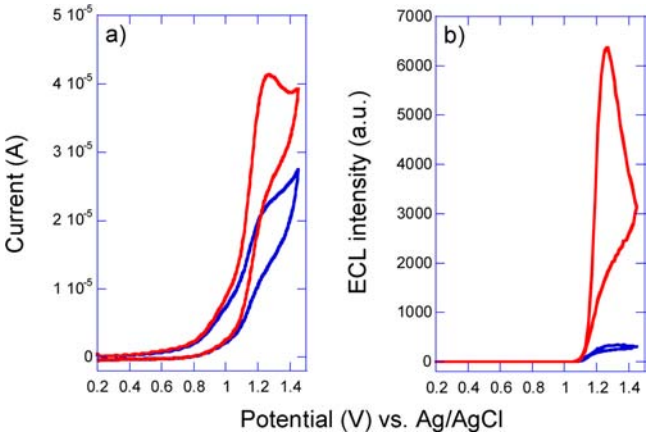

Figure 2. (a) Cyclic voltammetry and (b) ECL signal of pNIPAM-1 microgels in the swollen state at 25 °C (blue) and in the collapsed state at 37 °C (red). Experiments were performed on glassy carbon (GC) electrode in 20 mM PBS (pH 7.4) with 10 mM TPrA. The concentration of the ruthenium complex is 50 μM (i.e., 1 g/L of polymer). Scan rate: 50 mV s^{-1}.

irreversible anodic wave starting at 0.8 V is attributed to the oxidation of TPrA. A second anodic wave is observed at 1.2 V corresponding to the electrocatalytic oxidation of TPrA by the ruthenium centers.[14a,17] When heating the solution above the VPTT, the current of this second wave is increased by a ~1.7-fold factor, similarly to DPV experiments. ECL is emitted at 1.2 V where the ruthenium centers are oxidized but no ECL emission was detected at the oxidation potential of TPrA. This ECL pattern shows that the ECL mechanism does not involve the "revisited route", where TPrA radicals diffuse and react directly with $Ru(bpy)_3^{2+}$ to generate the excited state.[14b,18] Furthermore, the coreactant or its radicals have to gain access to the ruthenium sites to produce ECL. However, their diffusion is blocked or rendered more difficult within the collapsed microgels, and one would expect a decrease of the ECL intensity. Indeed, the diffusion coefficient of redox species in the collapsed gels is ~2 orders of magnitude smaller than in the swollen gels.[19] Therefore, considering the diffusion of the coreactant to the ruthenium centers, we expect that ECL is mainly emitted in the shell of the microgels when they are in the collapsed state.

The phase transition event has a drastic effect on the ECL emission of pNIPAM-1 (Figures 2b and S4a, Supporting Information). ECL intensity is remarkably increased with gel collapse. It rises at the VPTT and then remains constant. Such an intriguing behavior is the opposite of what one would expect considering blocked diffusion inside the collapsed microgels. An interesting observation from Figure 2b is the calculation of an enhancement factor for the ECL intensity. It is defined as the ratio of the ECL intensity measured just below and above the VPTT so it reflects the effect of the swell−collapse transition. The enhancement factor for pNIPAM-1 is calculated when temperature is increased from 31 to 35 °C, and it gives an enhancement factor of 26. This large enhancement is much higher than the current increase, and it occurs at the VPTT. We compared this value with the ECL of a free $Ru(bpy)_3^{2+}$ solution with TPrA, which is considered as an ECL reference for the studied system. In this case, the ECL intensity is just increased by a factor 1.6 for the same variation of temperature (Figure S5, Supporting Information).[20] The ECL enhancement of the microgels is thus much higher than those of the reference ECL system. DBAE and oxalate were also used as coreactant, and the calculation gives an enhancement factor of 17 and 48, respectively (Figures S6 and S7, Supporting Information). The ECL reversibility of the microgels was also investigated. ECL signal increases with the gel collapse and it decays to its initial value when temperature is switched back below its VPTT (Figure S4b, Supporting Information). ECL intensity is reversibly cycled between low and enhanced values upon the microgel transition.

To further analyze the ECL behavior of the thermoresponsive microgels, we tested other samples with different VPTT (Table S1, Supporting Information). For the pNNPAM microgel, the diameter of the particles decreases from 160 to 100 nm when heated above its VPTT, which is 20 °C. We measured a 16-fold amplification factor for the ECL intensity at the VPTT using TPrA as coreactant (Figure 3b). For the pNIPAM/pNIPMAM, the enhancement factor was 17 when the diameter of the particles decreases from 195 to 105 nm at its VPTT. For all the tested microgels, ECL enhancement correlates with the collapse of the microgels at their respective VPTT.

We studied also the influence of the amount of ruthenium complex covalently attached into the microgel particles. By increasing the concentration of the Ru monomer in the feed during the polymerization, we obtained microgel particles of pNIPAM containing 3.3-fold higher concentration of ruthenium complex compared to pNIPAM-1 (Table S1, Supporting Information). The VPTT of this new pNIPAM-2 sample is identical to pNIPAM-1 (i.e., 33 °C). Although the microgel sizes were similar (Figure 3a), the ECL enhancement factor of

dx.doi.org/10.1021/ja401011j | J. Am. Chem. Soc. 2013, 135, 5517−5520

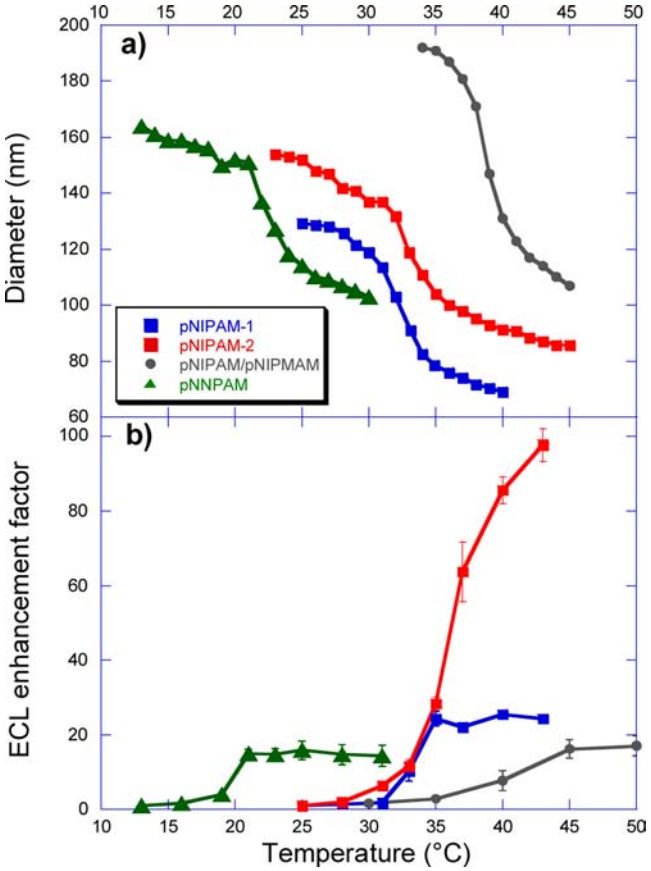

Figure 3. Influence of temperature on (a) the diameter and on (b) the ECL for the different microgels in identical experimental conditions. The size of the microgels is determined by DLS. ECL is measured during voltammetric experiments on GC electrode in 20 mM PBS solution (pH 7.4) with 10 mM TPrA. The ruthenium concentration is 3.7×10^{-5} M in the different microgels. ECL enhancement factor is calculated by normalizing ECL intensity by the ECL value measured just below VPTT for each microgel.

pNIPAM-2 is much higher than those of pNIPAM-1 (Figure 3b). Indeed, ECL intensity is amplified by 98-fold after the VPTT. This huge enhancement is directly related to the higher amount of ruthenium complex in pNIPAM-2 compared to pNIPAM-1.

All the prepared microgels provide a strong enhancement of the ECL emission in the collapsed state. This amplification correlates directly with the VPTT for each microgel (Figure 3). The experimental results show that this ECL enhancement is not related to the quantum yield of PL since VPTT has no particular effect on the PL intensity (Figure S1, Supporting Information). Therefore the electron-transfer processes inducing the excited state of the luminophore are the key phenomena leading to this huge enhancement.

The collapse occurring at the VPTT provokes the decrease of the average distance between adjacent ruthenium centers in the microgels and also an important dehydration corresponding to a hydrophilic−hydrophobic transition. ECL is a process that depends highly on the electrode material, on the oxidation rate of the coreactant and on the stability of its radicals.[14] For example, ECL emission is more intense in presence of surfactants, which renders the electrode surface hydrophobic.[18,21] Therefore, the more hydrophobic environment created locally by the microgel collapse may increase the ECL efficiency. Another possibility in order to interpret the ECL amplification is related to the smaller average distance between the ruthenium sites, which occurs above VPTT. To test the influence of this parameter, we plotted the normalized ECL intensity as a function of the average distance between ruthenium sites for the different microgels (Figure 4). As a

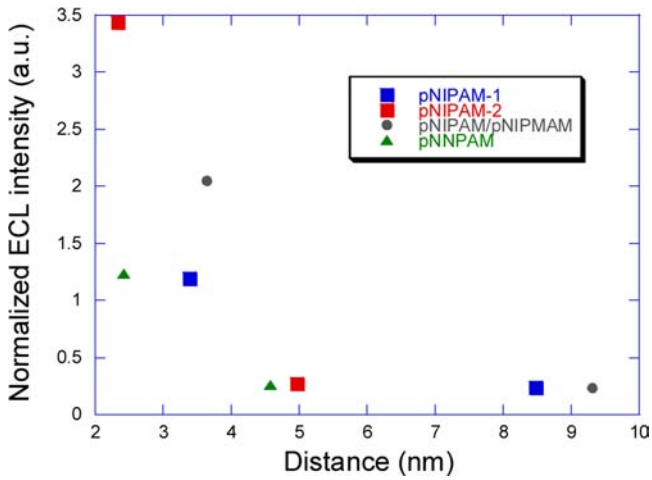

Figure 4. Variation of the normalized ECL intensity with the average distance between adjacent ruthenium sites in the microgels. Since VPTT of the different microgels are different, ECL intensities were normalized by the ECL values measured with the reference system (i.e., free $Ru(bpy)_3^{2+}$/TPrA) for each temperature.

first approximation,[22] we considered that the ruthenium centers are randomly distributed within the polymer networks. For pNIPAM-1, the values are 8.5 and 3.4 nm in the swollen and collapsed states, respectively. One can observe a general trend with a sharp increase of the ECL intensity when intersites distance decays (Figure 4).

The distance between adjacent redox sites is the key factor governing the efficiency of the electron-transfer processes in the microgels. It is equivalent to the charge diffusion in redox polymers involving an electron-hopping process from site to site where transport of both electrons and charge-compensating counterions occurs simultaneously.[23] The rate k of electron transfer decays exponentially with the distance r between the redox centers in the transition state. The distance dependence of the rate constant for electron-transfer is given by $k \alpha \exp(-r/\gamma)$. The self-exchange rate constant $k_{sol} \approx 10^9$ M^{-1} s^{-1} has been reported for the $[Ru(bpy)_3^{2/3+}]$ system in water.[24] The factor γ is function of the height of the energy barrier, and it can be considered as the attenuation factor per unit of distance. In hydrogels, electron-transferring collisions are effective when the distance between the oxidized and reduced redox centers is in the 1−3 nm range.[23] This corresponds to the typical distance calculated for the different microgels in the collapsed state where ECL increases drastically (Figure 4). Indeed, the values are distributed between 2.3 and 3.6 nm for the different microgels above the VPTT. The natural inference is that microgel collapse enhances considerably the ECL signal by decreasing the intersites distance, even if dehydration may play also an important role in the mechanism.

The decrease of this intersite distance increases the rate of the electron-exchange reactions between ruthenium sites in the microgels. These electron-exchange reactions are involved in two redox processes occurring in the microgels, which may

dx.doi.org/10.1021/ja401011j | J. Am. Chem. Soc. 2013, 135, 5517−5520

explain the observed ECL enhancement. As already mentioned, it favors, on the one hand, the electron-hopping process between the ruthenium sites, which enhances the electrocatalytic oxidation of the coreactant. On the other hand, a second effect contributing to this enhancement could be the formation of $Ru(bpy)_3^{+}$ and of $Ru(bpy)_3^{3+}$ in the microgels in close enough proximity so that ECL annihilation occurs.[1a] It is well-known that the annihilation reaction between $Ru^{(I)}(bpy)_3^{+}$ and $Ru^{(III)}(bpy)_3^{3+}$ generates the MLCT excited state.[1a] In the microgels, Ru(III) is produced in the shell by oxidation at the electrode surface. The Ru(I) form could be generated by the highly reducing radicals of oxalate and amine-based coreactants (i.e., TPrA and DBAE) following different pathways.[14b,16a] Even if $Ru(bpy)_3^{+}$ is unstable in aqueous solution,[16b] it has been reported that its lifetime is long enough in water to react with the $Ru(bpy)_3^{3+}$ form at the micrometric scale to generate the ECL emission.[25] The duration of its lifetime may be even longer in the hydrophobic environment of the collapsed state and thus increases the ECL signal. Decreasing the average distance between the ruthenium sites increases then the rate of the annihilation reaction leading to the enhanced ECL emission.

In this work, an amplification of the ECL intensity in thermoresponsive microgels was discovered. ECL signals are enhanced up to 2 orders of magnitude, and this reversible phenomenon correlates with the swell−collapse transition of the microgels. It is noteworthy that this turn-on signal with increasing temperature is extremely rare with other thermoresponsive luminescent systems. Moreover, this unique characteristic is not available in molecular systems. This unexpected behavior is related to the microgel shrinking, which decreases the average distance between adjacent redox sites. The decrease of this distance favors both charge diffusion by electron-hopping in the microgels and also the ECL annihilation mechanism. Both effects contribute to the observed ECL enhancement. Our original approach could be extended to other types of stimuli in order to design new ultrasensitive assays taking advantage of bioresponsive microgels[26] and also to exploit their unique properties as labels in immunoassays and in enzymatic assays. In addition, such ECL enhancement related to the distance dependence offers also the opportunity to develop tunable ECL resonance energy-transfer nanomaterials for multicolor emission.

■ ASSOCIATED CONTENT

Ⓢ Supporting Information

Details of synthesis and characterization. DPV, PL and ECL analysis. Supporting figures. Calculation of the average distance between ECL sites. This material is available free of charge via the Internet at http://pubs.acs.org.

■ AUTHOR INFORMATION

Corresponding Author

vravaine@enscbp.fr; sojic@enscbp.fr

Notes

The authors declare no competing financial interest.

■ ACKNOWLEDGMENTS

We acknowledge helpful discussions with Frédéric Kanoufi and Alexander Kuhn. Financial support has been received from CNRS and Conseil Régional d'Aquitaine.

■ REFERENCES

(1) (a) Bard, A. J. *Electrogenerated Chemiluminescence*; M. Dekker: New York, 2004. (b) Miao, W. *Chem. Rev.* **2008**, *108*, 2506−2553.

(2) (a) Swanick, K. N.; Ladouceur, S.; Zysman-Colman, E.; Ding, Z. *Angew. Chem., Int. Ed.* **2012**, *51*, 11079−11082. (b) Ding, Z.; Quinn, B. M.; Haram, S. K.; Pell, L. E.; Korgel, B. A.; Bard, A. J. *Science* **2002**, *296*, 1293−1297. (c) Swanick, K. N.; Hesari, M.; Workentin, M. S.; Ding, Z. *J. Am. Chem. Soc.* **2012**, *134*, 15205−15208. (d) Devadoss, A.; Dickinson, C.; Keyes, T. E.; Forster, R. J. *Anal. Chem.* **2011**, *83*, 2383−2387.

(3) (a) Hendrickson, G. R.; Lyon, L. A. *Soft Matter* **2009**, *5*, 29−35. (b) Peng, H. S.; Stolwijk, J. A.; Sun, L. N.; Wegener, J.; Wolfbeis, O. S. *Angew. Chem., Int. Ed.* **2010**, *49*, 4246−4249.

(4) Gota, C.; Okabe, K.; Funatsu, T.; Harada, Y.; Uchiyama, S. *J. Am. Chem. Soc.* **2009**, *131*, 2766−2767.

(5) Wang, D.; Liu, T.; Yin, J.; Liu, S. *Macromolecules* **2011**, *44*, 2282−2290.

(6) (a) Wu, W.; Zhou, T.; Shen, J.; Zhou, S. *Chem. Commun.* **2009**, 4390−4392. (b) Wu, W.; Shen, J.; Gai, Z.; Hong, K.; Banerjee, P.; Zhou, S. *Biomaterials* **2011**, *32*, 9876−9887. (c) Wu, W.; Shen, J.; Banerjee, P.; Zhou, S. *Adv. Funct. Mater.* **2011**, *21*, 2830−2839.

(7) (a) Wu, C.; Chiu, D. T. *Angew. Chem., Int. Ed.* **2013**, *52*, 3086−3109. (b) Vetrone, F.; Naccache, R.; Zamarrón, A.; Juarranz de la Fuente, A.; Sanz-Rodríguez, F.; Martínez Maestro, L.; Martín Rodriguez, E.; Jaque, D.; García Solé, J.; Capobianco, J. A. *ACS Nano* **2010**, *4*, 3254−3258. (c) McLaurin, E. J.; Vlaskin, V. A.; Gamelin, D. R. *J. Am. Chem. Soc.* **2011**, *133*, 14978−14980. (d) Albers, A. E.; Chan, E. M.; McBride, P. M.; Ajo-Franklin, C. M.; Cohen, B. E.; Helms, B. A. *J. Am. Chem. Soc.* **2012**, *134*, 9565−9568.

(8) (a) Bocharova, V.; Tam, T. K.; Halamek, J.; Pita, M.; Katz, E. *Chem. Commun.* **2010**, 2088−2090. (b) Tam, T. K.; Pita, M.; Motornov, M.; Tokarev, I.; Minko, S.; Katz, E. *Electroanalysis* **2010**, *22*, 35−40. (c) Balogh, D.; Tel-Vered, R.; Freeman, R.; Willner, I. *J. Am. Chem. Soc.* **2011**, *133*, 6533−6536.

(9) Álvarez-Puebla, R. A.; Contreras-Cáceres, R.; Pastoriza-Santos, I.; Pérez-Juste, J.; Liz-Marzán, L. M. *Angew. Chem., Int. Ed.* **2009**, *48*, 138−143.

(10) Karg, M.; Lu, Y.; Carbó-Argibay, E.; Pastoriza-Santos, I.; Pérez-Juste, J.; Liz-Marzán, L. M.; Hellweg, T. *Langmuir* **2009**, *25*, 3163−3167.

(11) Kano, M.; Kokufuta, E. *Langmuir* **2009**, *25*, 8649−8655.

(12) Suzuki, D.; Yoshida, R. *Macromolecules* **2008**, *41*, 5830−5838.

(13) Bowen, E. J.; Sahu, J. *J. Phys. Chem.* **1959**, *63*, 4−7.

(14) (a) Kanoufi, F.; Zu, Y.; Bard, A. J. *J. Phys. Chem. B* **2001**, *105*, 210−216. (b) Miao, W.; Choi, J.-P.; Bard, A. J. *J. Am. Chem. Soc.* **2002**, *124*, 14478−14485.

(15) Liu, X.; Shi, L.; Niu, W.; Li, H.; Xu, G. *Angew. Chem., Int. Ed.* **2007**, *46*, 421−424.

(16) (a) Kanoufi, F.; Bard, A. J. *J. Phys. Chem. B* **1999**, *103*, 10469−10480. (b) Rubinstein, I.; Bard, A. J. *J. Am. Chem. Soc.* **1981**, *103*, 512−516.

(17) Zu, Y.; Bard, A. J. *Anal. Chem.* **2000**, *72*, 3223−3232.

(18) Chen, Z.; Zu, Y. *J. Phys. Chem. C* **2009**, *113*, 21877−21882.

(19) Zhang, W.; Gaberman, I.; Ciszkowska, M. *Anal. Chem.* **2002**, *74*, 1343−1348.

(20) (a) Wallace, W. L.; Bard, A. J. *J. Phys. Chem.* **1979**, *83*, 1350−1357. (b) Gonzalez-Velasco, J. *J. Phys. Chem.* **1988**, *92*, 2202−2207.

(21) (a) Zu, Y.; Bard, A. J. *Anal. Chem.* **2001**, *73*, 3960−3964. (b) Cole, C.; Muegge, B. D.; Richter, M. M. *Anal. Chem.* **2003**, *75*, 601−604.

(22) Lu, Y. *Photochem. Photobiol. Sci.* **2010**, *9*, 392−397.

(23) Heller, A. *Curr. Opin. Chem. Biol.* **2006**, *10*, 664−672.

(24) Sutin, N.; Creutz, C. *Pure Appl. Chem.* **1980**, *52*, 2717.

(25) Fiaccabrino, G. C.; Koudelka-hep, M.; Hsueh, Y.-T.; Collins, S. D.; Smith, R. L. *Anal. Chem.* **1998**, *70*, 4157−4161.

(26) Hendrickson, G. R.; Andrew Lyon, L. *Soft Matter* **2009**, *5*, 29−35.